29th International Cosmic Ray Conference Pune (2005) **00**, 101–104

Angular Resolution of the Pierre Auger Observatory

C. Bonifazi for Pierre Auger Collaboration
Pierre Auger Observatory, Av. San Martín Norte 304, (5613) Malargüe, Argentina
Presenter: C. Bonifazi (bonifazi@cbpf.br), bra-bonifazi-C-abs1-he14-oral

We studied the angular resolution of the Pierre Auger Detector using data collected from January 2004 to May 2005. The detector consists of two independent components, the fluorescence detector and the surface detector. Hybrid events, observed simultaneously by both components, have smaller reconstruction uncertainties than the events observed with only one component. The hybrid resolution is extracted from artificial showers generated by laser shots, while the surface detector angular accuracy is then determined from the comparison of the hybrid geometrical fit with the one obtained from the surface detector alone. We used adjacent surface detector stations to cross check our methods. The angular reconstruction accuracy of the surface detector events is given as a function of station multiplicity.

1. Introduction

The Pierre Auger Observatory consists of two independent components, the fluorescence detector (FD) and the surface detector (SD) [1]. We have determined the angular resolution of events recorded by the surface detector alone, where we have the largest statistics, and of events recorded by both components, the hybrid events, where we have the highest accuracy. We define the angular resolution as the angular radius that would contain 68% of showers coming from a point source, which is approximately 1.5 times the σ parameter coming from the Gaussian resolution function.

The hybrid resolution is extracted from artificial showers generated by laser shots in the center of the array (section 2). The SD stations timing uncertainty is directly modeled from the data and adjusted using two pairs of adjacent stations located in the surface array (section 3). Using this model the geometrical parameters uncertainty is then directly extracted from our minimization procedure (section 4). The SD angular resolution is estimated by comparing the hybrid angular reconstruction and the SD-only reconstruction for those hybrid events that have 3 or more triggered stations (section 5).

2. Hybrid Resolution

To extract the angular resolution of the hybrid events, artificial showers were generated by laser shots. The Central Laser Facility (CLF), located in the middle of the array at about 30 km from each fluorescence detector, contains a remotely controlled laser, which produces vertical showers (within 0.01°). At the same time it sends a pulse of light to a surface station to generate an artificial hybrid event [2]. The laser shot reconstruction is done with the same algorithm used to reconstruct real events with only one surface station [3]. From the studies of those artificial showers, the σ value obtained from the adjusted Gaussian resolution function ($\propto\ e^{-\Omega^2/2\sigma^2}$, where Ω is the angle between the reconstructed shower axis and the true one) is 0.2° (see figure 1), corresponding to 0.15° for the shower angle (χ_0) inside the shower detector plane (SDP, the plane that contains the shower axis and the FD telescope location) and 0.15° for the determination of the SDP itself [3]. This σ corresponds to an angular resolution of 0.3°. Also, the core location is determined with an uncertainty of 50 m, which is independent of the shower geometry. It is determined by the spacing of 1.5 km between the surface detectors and by the SD and FD synchronization, which is better than 100 ns [4].

The laser events have geometrical characteristics that are favorable (in relation to real hybrid events) for a better hybrid reconstruction of the geometry. The SDP determination is independent of the shower geometry, it only

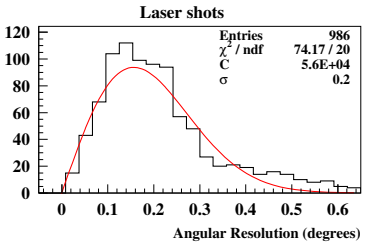

Figure 1. Distribution of the estimated angular uncertainty for laser shots. The σ value obtained is 0.2° (see text).

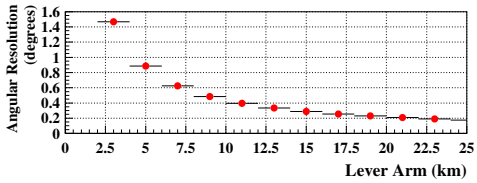

Figure 2. Expected angular uncertainties for real events as a function of the shower lever arm (see text).

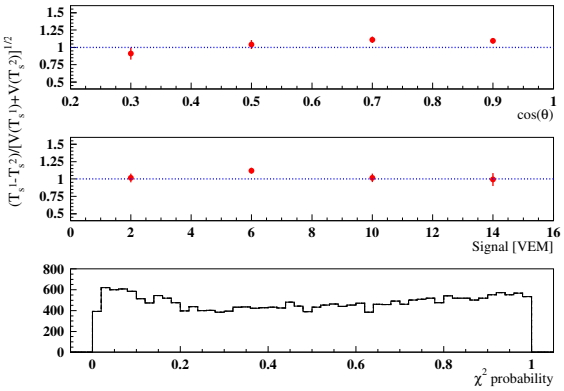

Figure 3. Average $(T_s^1 - T_s^2)/\sqrt{V(T_s^1) + V(T_s^2)}$ for doublets station inside a given event, as a function of the shower zenith angle (top) and the average signal in the doublet tanks (middle). The χ^2 probability distribution after the geometrical fit using a spherical shower front and our $V(T_s)$ model as adjusted on the doublet data (bottom).

depends on the number of triggered pixels in the camera. For a typical real shower (with a track length of 23°), the accuracy in the SDP is about 0.3°. However, the accuracy on χ_0 depends on the particular geometry of the shower with respect to the FD. Correcting for the mean distance of our real shower sample (5.8 km) and for the mean shower length in the camera (23°) we obtained an hybrid angular resolution of about 0.6°.

The hybrid angular resolution can also be estimated for real events using the corresponding shower geometry. Since the uncertainty in the reconstructed core is independent of the shower distance, the uncertainty of the hybrid shower axis can be roughly estimated as the ratio between the core uncertainty and the shower axis "lever arm", defined as the distance along the shower axis from ground to the point seen in the camera by the pixel with the highest elevation.

In figure 2 we show the expected hybrid accuracy as a function of the shower lever arm: notice that for a lever arm of 14 km corresponding to laser events, the expected angular uncertainty is about 0.3°, consistent with the accuracy obtained from laser studies. The mean shower lever arm is about 7.5 km. Therefore, the mean accuracy for real hybrid events is about 0.6°.

3. Time Variance Model

The angular accuracy of the SD events is driven by the accuracy with which one can measure the time of arrival (T_s) of the shower front in each station. The time T_s in each station is determined by the GPS system and the internal clock in the electronics which determines the timing bin in the Flash Analog-to-Digital Converters (FADC) traces. The timing accuracy is $\sim$8 ns [1]. Modeling T_s as the time of arrival of the first particle out of a set of n particles arriving in a time interval ΔT, the variance of T_s, $V(T_s)$, is given by:

$$V(T_s) = \frac{n\,\Delta T^2}{(n+1)^2\,(n+2)} + b^2 \simeq (a\,T_{50}/S_{VEM})^2 + b^2$$

where b^2 models the irreducible accuracy of our station timing system, S_{VEM} is the signal measured in the station in units of vertical equivalent muons (VEM) [5], T_{50} is the time interval that contains the first 50% of the total signal as measured by the photomultiplier FADC traces, and a is a constant to be adjusted.

Two pairs of adjacent surface detector stations ("doublets") located within 11 meters from one another were used to adjust the above model to our measurements. For each shower that triggered a doublet (representing 1711 reconstructed events) we computed the T_s difference in each doublet and compared it with our modelled $V(T_s)$ adding a global correction for the zenith angle dependence (the shower front is better defined at large zenith angles than for vertical showers). We obtained the following parameterization:

$$V(T_s) = \left[(1.2\ T_{50}/S_{VEM})^2 + 600\ ns^2\right]\ (0.4 + 1.2\ \cos\theta).$$

We show in figure 3 the average ratio between the time difference $(T_s^1 - T_s^2)$ within a doublet and the associated uncertainty as derived from our model. In the top of the figure we show the evolution of the ratio as a function of zenith angle and in the middle as a function of the doublet average signal. In both cases, it is constant and close to unity, which shows that our $V(T_s)$ model is in good agreement with the experimental data.

We implemented this model in our geometrical estimation routine that describes the front of the shower as a perfect sphere. In figure 3 (bottom) we have plotted the χ^2 probability distribution of our minimizations for all the events with 4 stations or more passing the Auger quality cuts (our T5 selection) [6]. This distribution is almost flat as it should be in the ideal case. With such a distribution we have shown that both the geometrical reconstruction algorithm and the experimental uncertainty assigned in the fitting routine are well understood. The uncertainty given by the fitting procedure is therefore an appropriate measure of our angular accuracy.

4. Surface Detector Resolution

Given our understanding of the experimental uncertainties and our model of the shower front, the geometrical reconstruction allows to calculate directly the angular resolution (Ω) on an event by event basis from the reconstructed zenith angle (θ) and azimuth (ϕ) resolution, using the relation:

$$V(\Omega) = 1/2\ (V(\theta) + \sin^2(\theta)\ V(\phi)).$$

In figure 4 we show our angular resolution as a function of the zenith angle for various station multiplicities (circles: 3 stations, squares, 4 stations, triangles: 5 stations or more, which corresponds to a mean multiplicity of 6.6 stations). The station multiplicity corresponds roughly to an energy range of $E < 4$ EeV, $3 < E < 10$ EeV and $E > 8$ EeV respectively. As it can be seen, the angular resolution is 1.8° in the worst case of vertical showers with only 3 stations hit. This value improves significantly for 4 or more stations where our angular resolution is always better than 1.2°. Above 60 degrees the event multiplicity increases rapidly with zenith angle and only a few low energy events trigger only 3 stations, for which the accuracy decreases.

5. Surface Detector only and Hybrid Comparison

Hybrid events that trigger 3 detectors or more can be reconstructed using both the hybrid and the SD-only mode, giving two independent estimates of the geometry. The comparison of these estimates is therefore a check of our angular resolution. In figure 5 we show the space-angle difference between these two estimates for showers with exactly 3 stations and for two different zenith angles cuts ($0^\circ < \theta < 30^\circ$ and $30^\circ < \theta < 50^\circ$) as well as for showers with 4 stations and 5 or more stations. In the adjusted Gaussian resolution function (as was shown in section 2), the σ parameter is larger than for the one expected from SD alone. For the 3-fold case, with $0^\circ < \theta < 30^\circ$, the σ parameter from the comparison between hybrid and surface reconstruction is

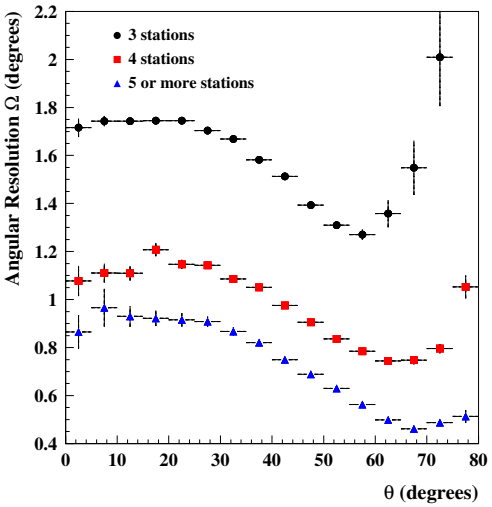

Figure 4. Angular resolution for the surface detector as a function of the zenith angle (θ) for various stations multiplicities: circles 3 stations (approx. $E < 4$ EeV), squares 4 stations (approx. $3 < E < 10$ EeV) and triangles more than 4 stations (approx. $E > 8$ EeV).

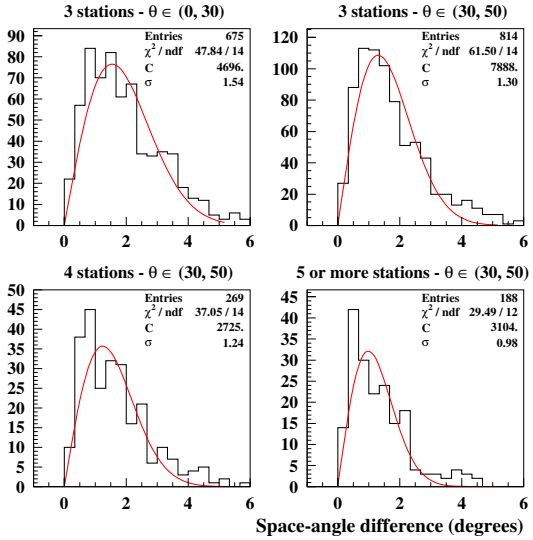

Figure 5. Comparison between hybrid and SD-only geometrical reconstruction. Top, for 3 stations with two zenith angle ranges $0^\circ < \theta < 30^\circ$ and $30^\circ < \theta < 50^\circ$. Bottom left, 4 stations, bottom right 5 stations or more, both with $30^\circ < \theta < 50^\circ$.

$\sim 1.5^\circ$. Considering a σ of 0.4° for hybrid events, with this method we obtain a σ for the surface detector of 1.4°, while for the direct method (see section 4) it is approximately 1.2°. This difference could be due to the fact that a large range of zenith angles must be considered in order to have enough statistics, implying that different angular resolutions are mixed in a single range. The large χ^2 values in the fit could be an indication of this mixing. More work is needed in this area to fully understand this difference.

6. Conclusions

The angular resolution was determined experimentally for both hybrid and surface detector only reconstructions. The angular resolution for hybrid events is about 0.6°, while the surface detector angular resolution was found to be better than 2.2° for 3-fold events ($E < 4$ EeV), better than 1.7° for 4-folds events ($3 < E < 10$ EeV) and better than 1.4° for higher multiplicity ($E > 8$ EeV).

References

[1] J. Abraham *et al.*, Pierre Auger Collaboration, Nucl. Intr. Meth. A523, (2005), 50
[2] F. Arqueros *et al.*, Pierre Auger Collaboration, 29th ICRC Pune (2005), usa-malek-M-abs1-he15-poster
[3] Pierre Auger Collaboration, 29th ICRC Pune (2005), usa-mostafa-M-abs1-he14-oral
[4] P. Allison *et al.*, Pierre Auger Collaboration, 29th ICRC Pune (2005), usa-covault-C-abs2-he15-poster
[5] M. Aglietta *et al.*, Pierre Auger Collaboration, 29th ICRC Pune (2005), usa-allison-PS-abs1-he14-poster
[6] D. Allard *et al.*, Pierre Auger Collaboration, 29th ICRC Pune (2005), usa-bauleo-PM-abs1-he14-poster